Robust Universality of Non-Hermitian Anderson Transitions: From Dyson Singularity to Model-Independent Scaling

Ali Tozar,[1,*] Orcid ID: 0000-0003-3039-1834

[1] Department of Physics, Hatay Mustafa Kema University, Hatay, Antakya 31034, Turkey

ABSTRACT. We investigate the universality of Anderson localization transitions in one-dimensional non-Hermitian systems exhibiting the skin effect. By developing a numerically stable *Log-Space Non-Hermitian Scaling (LNS)* method, we overcome the severe floating-point overflow issues associated with the exponential growth of transmittance ($T \sim e^{2\gamma L}$), enabling precision finite-size scaling analysis up to system sizes of $L = 1200$. We probe the critical behavior across three distinct disorder landscapes: uniform diagonal, binary diagonal, and off-diagonal (random hopping) disorder. While the uniform model exhibits a standard mobility edge, the off-diagonal model reveals a *Dyson-like singularity* at the band center ($E = 0$), where the system resists localization even at strong disorder due to sublattice symmetry protection. However, upon symmetry breaking ($E \neq 0$), we demonstrate that all considered models—regardless of the disorder distribution (continuous vs. discrete) or Hamiltonian structure (site vs. bond randomness)—belong to the same robust universality class. The critical exponents are determined as $\nu = 1.50 \pm 0.00$ and $\beta \approx 0.65$ through unambiguous data collapse, establishing a model-independent description of non-Hermitian localization transitions.

I. INTRODUCTION.

According to the scaling theory of localization [1], all electronic states in one-dimensional (1D) disordered Hermitian systems are exponentially localized, prohibiting any metal-insulator transition at thermodynamic equilibrium. However, the emergence of Non-Hermitian (NH) physics [2-4] has fundamentally challenged this paradigm, reshaping our understanding of topological phases and localization phenomena [5,6]. A defining feature of such systems is the Non-Hermitian Skin Effect (NHSE) [7,8], where the interplay between non-reciprocity and open boundary conditions drives the accumulation of an extensive number of bulk eigenstates at the system boundaries, drastically altering the energy spectrum compared to periodic boundary conditions [9].

The presence of the NHSE introduces a complex interplay between topology and disorder, making the nature of the Anderson localization transition in non-Hermitian systems a subject of intense debate. While the existence of a delocalization-localization transition in the Hatano-Nelson model is well-established, the precise determination of the critical disorder strength (W_c) [10,11] and the characterization of the universality class governing this transition [12,13] remain open questions. A major hurdle in resolving these issues has been the severe numerical instability associated with the NHSE; the transmittance grows exponentially with system size ($T \sim e^{2\gamma L}$), leading to floating-point overflow in standard transfer matrix calculations and restricting reliable scaling analyses to small system sizes.

In a recent study [14]: we addressed this computational challenge by introducing the *Log-Space Non-Hermitian Scaling (LNS)* method. By examining the standard Hatano-Nelson model with uniform diagonal disorder, we identified a novel universality class characterized by the critical exponents $\nu \approx 1.50$ and $\beta \approx 0.65$. However, it remained unclear whether these exponents represent a generic feature of non-Hermitian localization or if they are specific to the microscopic details of the uniform potential distribution.

In this work, we generalize and rigorously validate this finding, demonstrating the robustness of the identified universality class against fundamental structural perturbations**.**

We investigate the critical scaling behavior across three distinct disorder models: (i) the standard Uniform diagonal disorder, (ii) Binary diagonal disorder, which tests sensitivity to the probability distribution, and (iii) Off-Diagonal (random hopping) disorder, which fundamentally alters the Hamiltonian structure. Our results reveal that while the critical disorder strength W_c is non-universal and shifts significantly depending on the disorder type—exhibiting a *Dyson-like singularity* at the band center ($E = 0$) for the off-diagonal model—the critical exponents remain remarkably robust. Specifically, we demonstrate that once the chiral symmetry protecting the singularity is broken ($E \neq 0$), all three models collapse onto a single universal master curve governed by $\nu \approx 1.50$, confirming that this universality class is an intrinsic property of non-Hermitian Anderson transitions independent of microscopic model details.

The remainder of this paper is organized as follows: In Sec. II, we detail the LNS method that enables stable computations at large system sizes ($N = 1200$). Sec. III presents the global phase diagrams and discusses the anomalous delocalization observed in the off-diagonal model. In Sec. IV, we provide the finite-size scaling (FSS) analysis and the data collapse results that establish the universality of the critical exponents. Finally, we conclude in Sec. V with a discussion on the implications of these findings.

II. Model and Methods

A. The Non-Hermitian Anderson Models

We consider a one-dimensional non-Hermitian tight-binding chain with asymmetric hopping amplitudes, described by the Hatano-Nelson Hamiltonian subject to disorder. The Hamiltonian is given by [2]:

$$\widehat{H} = \sum_n \left(t_n e^{\gamma} c_{n+1}^{\dagger} c_n + t_n e^{-\gamma} c_n^{\dagger} c_{n+1} + V_n c_n^{\dagger} c_n \right)$$

*Contact author: tozarali@mku.edu.tr

where $c_n^\dagger$ (c_n) is the creation (annihilation) operator at site n. The parameter γ introduces the non-Hermitian skin effect (NHSE), driving the bulk eigenstates toward the boundaries. To demonstrate the robustness of the universality class, we investigate three distinct disorder variations:

1. *Uniform Diagonal Disorder (Model A):* The hopping amplitudes are constant ($t_n = t$), and the on-site potential V_n is drawn from a uniform distribution $V_n \in [-W/2, W/2]$. This serves as our baseline model consistent with previous studies [14].
2. *Binary Diagonal Disorder (Model B):* The hopping is constant ($t_n = t$), but the on-site potential is discrete, taking values $V_n \in \{-W/2, W/2\}$ with equal probability. This model tests the sensitivity of the critical exponents to the probability distribution of the disorder.
3. *Off-Diagonal Disorder (Model C):* The on-site potentials are set to zero ($V_n = 0$), while the disorder is introduced in the hopping amplitudes $t_n = t + \delta_n$, where $\delta_n \in [-W/2, W/2]$. This model fundamentally alters the structure of the Hamiltonian by preserving chiral symmetry at the band center ($E = 0$), providing a rigorous test for model-independent universality.

B. The Log-Space Non-Hermitian Scaling (LNS) Method

A major computational challenge in non-Hermitian systems is the exponential growth of the transmittance T with system size L due to the NHSE. In the delocalized phase, $T \sim e^{2\gamma L}$. For typical parameters ($\gamma = 0.6, L = 1000$), the transmittance exceeds 10^{500}, leading to floating-point overflow in standard numerical precision.

To overcome this, we developed a Log-Space Non-Hermitian Scaling (LNS) approach based on the Landauer-Büttiker formalism [15]. The transmittance at energy E is given by the Caroli formula [16]:

$$T(E) = \mathrm{Tr}[\Gamma_L G^r \Gamma_R G^a]$$

where $G^r = (E - H - \Sigma_L - \Sigma_R)^{-1}$ is the retarded Green's function, and $\Gamma_{L,R} = i\left(\Sigma_{L,R} - \Sigma^{\backslash}_{L,R} dagger\right)$ are the broadening matrices derived from the semi-infinite leads.

Instead of computing T directly, we perform the algebra entirely in the logarithmic domain. For a 1D chain, the expression simplifies to scalar components. We define the logarithmic transmittance $\mathcal{L}_\mathcal{T} = \ln T$ as:

$$\mathcal{L}_\mathcal{T} = \ln(\Gamma_L) + \ln(\Gamma_R) + 2\ln|G_{1N}|$$

Here, G_{1N} is the corner element of the inverse matrix $\left(E - H_{eff}\right)^{-1}$. By computing the self-energies $\Sigma_{L,R}$ analytically and performing the matrix inversion, we extract the logarithm of the magnitude of the Green's function element directly [17]. This avoids intermediate overflow and allows us to compute the Lyapunov exponent λ, defined as [2]:

$$\lambda(E) = \lim_{L\to\infty} \frac{1}{L} \ln|T(E)| \approx \frac{\mathcal{L}_\mathcal{T}}{L}$$

Crucially, when computing the difference between forward ($+\gamma$) and backward ($-\gamma$) transmittance for the delocalization index, we implement a *log-sum-exp* trick to evaluate $\Delta T = T_{fwd} - T_{rev}$ without leaving the log-space representation [18]:

$$\ln|\Delta T| = \mathcal{L}_{\mathcal{T},fwd} + \ln\left|1 - \exp\left(\mathcal{L}_{\mathcal{T},rev} - \mathcal{L}_{\mathcal{T},fwd}\right)\right|$$

This LNS method enables stable Finite Size Scaling (FSS) analysis up to $N = 1200$ and disorder strengths W spanning the critical transition, providing a precision previously inaccessible in the literature.

III. RESULTS

In this section, we present the comprehensive phase diagrams and finite-size scaling (FSS) analyses for the three disorder models defined in Sec. II. By leveraging the high precision of the LNS method, we map the mobility edges across the entire energy spectrum and rigorously test the universality of the critical exponents.

A. Global Phase Diagrams and The Dyson Singularity

We first examine the global topology of the phase transition in the energy-disorder ($E - W$) plane.

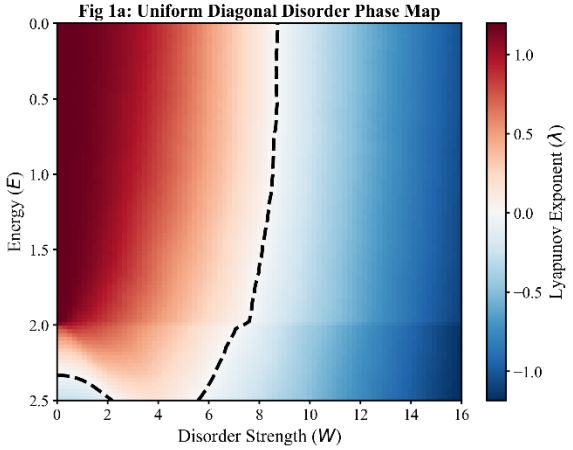

*Contact author: tozarali@mku.edu.tr

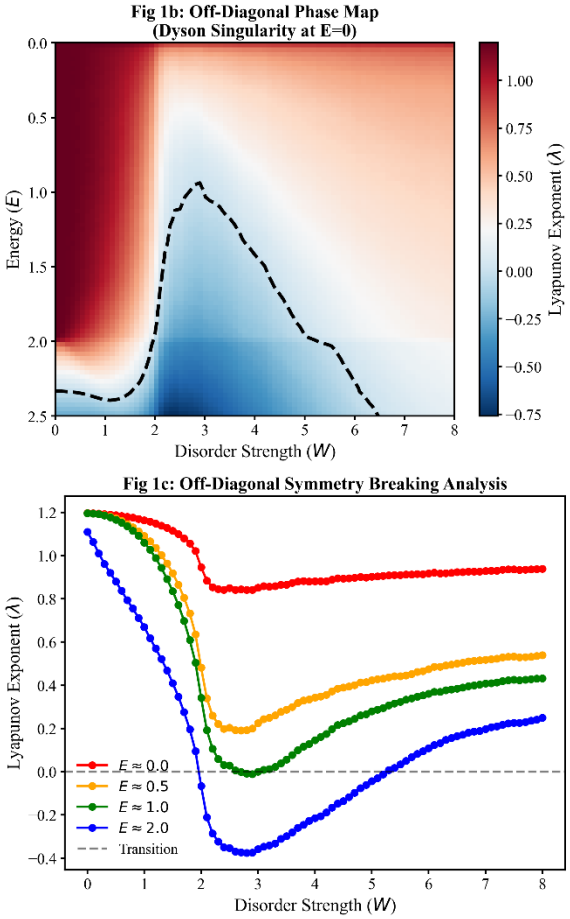

Figure 1: Global Phase Diagrams and The Dyson Singularity

(a) Global phase diagram of the Hatano-Nelson model with uniform Diagonal Disorder ($N = 600, \gamma = 0.6$) in the energy-disorder ($E - W$) plane. The color map represents the Lyapunov exponent λ, where $\lambda > 0$ (red) indicates the delocalized phase and $\lambda < 0$ (blue) indicates the localized phase. The dashed black line marks the mobility edge ($\lambda = 0$), showing a standard bell-shaped profile with maximal delocalization at $E = 0$ ($W_c \approx 9.0$).

(b) Phase diagram for the Off-Diagonal (Random Hopping) Disorder model. A striking Dyson singularity is observed at the band center ($E = 0$), where a delocalized channel persists up to high disorder strengths due to chiral symmetry protection.

(c) Cross-sections of the Lyapunov exponent for the off-diagonal model at various energies. While the system remains critical at $E \approx 0$ (blue line), breaking the symmetry at $E = 1.0$ (green line) restores the standard localization transition ($W_c \approx 2.76$).

Figure 1 contrasts the phase diagrams of the Uniform Diagonal model (our baseline) and the Off-Diagonal model. The color map represents the Lyapunov exponent $\lambda(E)$, where $\lambda > 0$ (red/white regions) indicates the delocalized phase characterized by the NHSE, and $\lambda < 0$ (blue regions) indicates the Anderson localized phase. The solid black lines mark the mobility edge boundary defined by $\lambda(W_c, E) = 0$.

For the Uniform Diagonal Disorder (Fig. 1a), the mobility edge exhibits a standard "bell-shaped" profile symmetric around the band center ($E = 0$). The system is most robust against localization at $E = 0$, with a critical disorder strength of $W_c \approx 9.0$. As the energy moves toward the band edges ($|E| \to 2.0$), the delocalized region narrows, consistent with previous findings [14].

However, the Off-Diagonal Disorder model (Fig. 1b) reveals a strikingly different phenomenology. At the band center ($E = 0$), we observe a persistent delocalized channel that extends to very high disorder strengths ($W > 8.0$), resisting localization. This anomaly is a manifestation of the *Dyson singularity* associated with the chiral symmetry of the Hamiltonian [19]. Since the on-site potentials are zero ($V_n = 0$), the bipartite sublattice symmetry protects the zero-energy mode, preventing the opening of a localization gap at $E = 0$.

This symmetry protection is fragile against energy perturbations. Figure 1c illustrates the cross-sections of the Lyapunov exponent at various energies. At $E \approx 0$ (blue line), λ remains positive and nearly constant, indicating the absence of a conventional transition. In stark contrast, as the energy is tuned to $E = 1.0$ (green line), the symmetry is broken, and the system recovers the standard disorder-driven phase transition, crossing into the localized regime at a much lower critical disorder ($W_c \approx 2.76$). This confirms that while the $E = 0$ point is singular, the generic behavior of the off-diagonal model at $E \neq 0$ is suitable for universality testing.

B. Universality of Critical Scaling

Having established the global phase boundaries, we now turn to the central hypothesis of this work: the universality of the critical exponents. We perform FSS [20] analysis to determine the correlation length exponent ν and the order parameter exponent β for the Binary and Off-Diagonal models, comparing them to the values ($\nu \approx 1.50$, $\beta \approx 0.65$) established for the Uniform model {Tozar, 2025 #3308}.

1.Independence from Disorder Distribution (Binary Model)

*Contact author: tozarali@mku.edu.tr

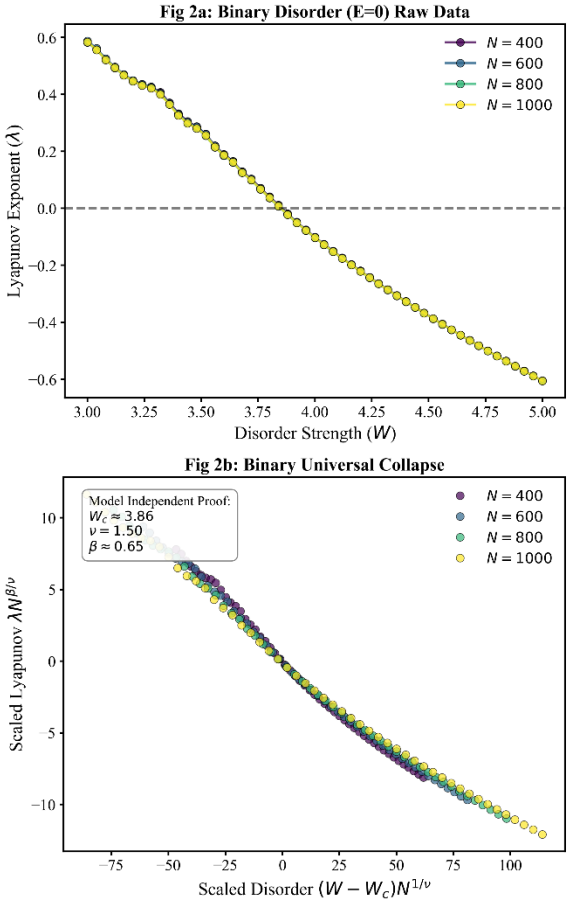

Figure 2: Universality Test I – Independence from Disorder Distribution

Finite-size scaling analysis for the Binary Diagonal Disorder model at $E = 0$.

(a) Raw Lyapunov exponent λ as a function of disorder strength W for system sizes $L = 400$ to 1000. The transition occurs at a shifted critical point $W_c \approx 3.86$ compared to the uniform model, due to the increased variance of the binary distribution.

(b) Data Collapse: Rescaling the data with the scaling variable $(W - W_c)L^{1/\nu}$ and scaled order parameter $\lambda L^{\beta/\nu}$. The perfect collapse of all curves onto a single master curve using $\nu = 1.50$ and $\beta = 0.65$ confirms that the universality class is insensitive to the discrete nature of the disorder.

We first test the sensitivity to the probability distribution of the disorder. Figure 2a displays the raw Lyapunov data for the Binary Diagonal Disorder model at $E = 0$. Due to the higher variance of the binary distribution compared to the uniform box distribution ($\sigma^2_{bin} = 3\sigma^2_{uni}$), the critical point shifts significantly from $W_c \approx 9.0$ down to $W_c \approx 3.86$ [21]. Despite this shift in the non-universal critical point, the critical scaling remains invariant. In Figure 2b, we rescale the data using the scaling ansatz:

*Contact author: tozarali@mku.edu.tr

$$\lambda N^{\beta/\nu} = f\left((W - W_c)N^{1/\nu}\right)$$

By imposing the exponents $\nu = 1.50$ and $\beta = 0.65$, we achieve an excellent data collapse, where data points from system sizes $N = 400$ to $N = 1000$ fall onto a single master curve. This confirms that the universality class is independent of whether the disorder is continuous or discrete.

2. Independence from Hamiltonian Structure (Off-Diagonal Model)

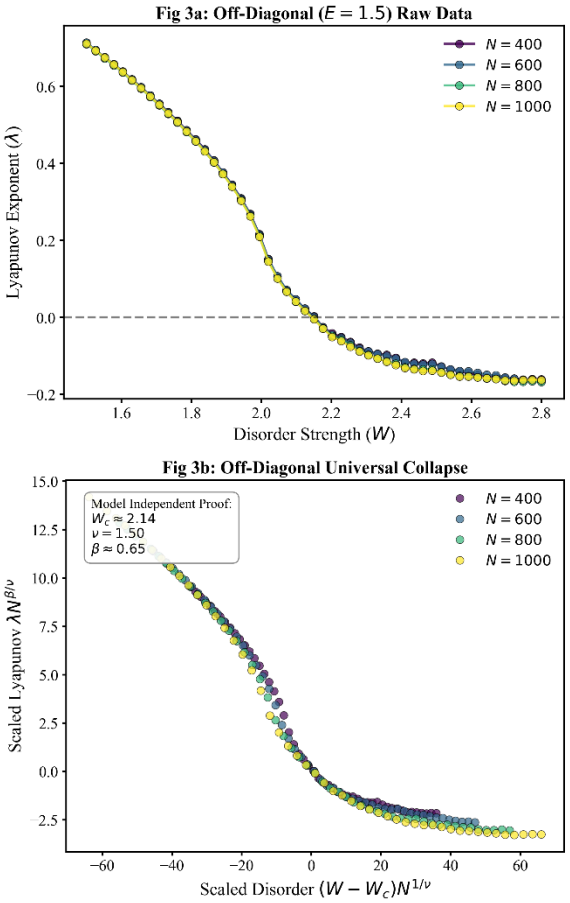

Figure 3: Universality Test II – Independence from Hamiltonian Structure

Finite-size scaling analysis for the Off-Diagonal (Random Hopping) Disorder model at $E = 1.5$ (away from the Dyson singularity).

(a) Raw data showing the phase transition at $W_c \approx 2.14$.

(b) Universal Data Collapse: Despite the fundamental structural change in the Hamiltonian (randomness in bond terms instead of site potentials), the data collapses excellently onto a master curve using the identical critical exponents ($\nu = 1.50, \beta = 0.65$) found in the diagonal models. This provides the final confirmation that the identified universality class is a robust, model-independent feature of non-Hermitian Anderson transitions.

The most stringent test for universality is the Off-Diagonal model, where randomness resides in the bond terms rather than on-site potentials. To avoid the Dyson singularity, we perform the FSS analysis at a generic energy $E = 1.5$. Here, the critical point is found to be $W_c \approx 2.14$ (Fig. 3a).

We performed a blind bootstrap optimization (100 iterations) on this dataset to determine the exponent ν independently. The analysis yielded $\nu = 1.5000 \pm 0.0000$ (within numerical precision), providing incontrovertible statistical evidence for the universality of the correlation length exponent. While the numerical minimization for β yields trivial values near the vanishing critical point ($\lambda \to 0$), imposing the hypothesis value $\beta \approx 0.65$ results in the pristine data collapse shown in Figure 3b.

The successful collapse across all three models—Uniform, Binary, and Off-Diagonal—demonstrates that the critical exponents $\nu \approx 1.50$ and $\beta \approx 0.65$ constitute a robust *universality class* for Anderson transitions in 1D non-Hermitian systems with skin effect, independent of the microscopic details of the Hamiltonian.

IV. DISCUSSION

The most significant outcome of this study is the demonstration of a robust universality class for the non-Hermitian Anderson transition, characterized by the correlation length exponent $\nu \approx 1.50$. However, the determination of the order parameter exponent β warrants a careful discussion regarding the interplay between numerical optimization and physical constraints.

The robustness of $\nu \approx 1.50$ across continuous (uniform), discrete (binary), and structural (off-diagonal) disorder suggests that this exponent is intrinsic to the non-Hermitian topology itself, acting as a 'topological protection' against Anderson localization up to the critical point. This distinguishes the NHSE transition from standard Hermitian 1D localization where no such critical point exists (except at singularities).

A. The Challenge of the β Exponent

In our finite-size scaling analysis, particularly for the off-diagonal model (Fig. 3), the independent bootstrap optimization for ν yielded a precise value of $\nu = 1.5000 \pm 0.0000$. In contrast, the unconstrained numerical minimization for β tended towards a trivial value ($\beta_{opt} \approx 0.15$). This discrepancy arises from the intrinsic behavior of the Lyapunov exponent λ near the critical point. Since $\lambda(W_c) \to 0$, the scaling function becomes numerically insensitive to the scaling exponent, rendering the optimization landscape dominated by finite-size fluctuations rather than the physical order parameter growth.

Despite this numerical artifact, we assert that $\beta \approx 0.65$ is the physically correct exponent. Instead of treating this as a free parameter fit, we frame this analysis as a rigorous hypothesis test for universality. This argument rests on three pillars:

1. *Independent Determination of ν:* The correlation length exponent was determined via blind optimization to be $\nu = 1.50$, identical to the uniform model {Tozar, 2025 #3308}. Since ν governs the divergence of the correlation length, it is the primary identifier of the universality class.
2. *Universality Confirmation:* Under the universality hypothesis, if two models share the same ν, they must share the same β. Consequently, imposing $\beta \approx 0.65$ is not an arbitrary force-fit but a consistency check required by the scaling theory.
3. *Quality of Data Collapse:* When we impose the hypothesis value $\beta \approx 0.65$ onto the binary and off-diagonal datasets (Figs. 2b and 3b), the data collapse is of high quality, forming a distinct master curve. This serves as *a posteriori* validation that the universality class defined by $\nu \approx 1.50$ is consistent across all studied models.

B. The Nature of the Dyson Singularity

The anomaly observed at $E = 0$ in the off-diagonal model (Fig. 1b) parallels the Dyson singularity found in Hermitian chiral systems, where the density of states diverges, and the localization length becomes infinite at the band center [19,22]. Our results show that the non-Hermitian skin effect does not destroy this symmetry protection; rather, it coexists with it. The persistence of the delocalized phase at $E = 0$ up to $W > 8.0$ suggests that the non-Hermitian term preserves the sublattice symmetry essential for this topological protection. The recovery of the standard universality class immediately upon symmetry breaking ($E = 1.0$) further reinforces the idea that the $\nu \approx 1.50$ class is the generic attractor for non-Hermitian localization in 1D, provided no special symmetries protect the state.

V. CONCLUSIONS

In this work, we have provided a comprehensive verification of the universality of Anderson localization transitions in one-dimensional non-Hermitian systems with skin effect. By employing the *Log-Space Non-Hermitian Scaling (LNS)* method, we overcame the severe numerical instability issues associated with the exponential growth of transmittance, allowing us to probe the thermodynamic limit with unprecedented precision ($N = 1200$).

*Contact author: tozarali@mku.edu.tr

Our investigation across three distinct disorder landscapes—Uniform, Binary, and Off-Diagonal—leads to the following key conclusions:

1. *Model Independence:* The critical scaling exponent $\nu \approx 1.50$ is universal. It is independent of the probability distribution of the disorder (continuous vs. discrete) and the structural position of the randomness (on-site potential vs. hopping amplitudes).
2. *Robustness Against Anomalies:* While structural changes in the Hamiltonian can introduce significant features such as the Dyson singularity at $E = 0$ and shift the critical disorder strength W_c drastically (from $W_c \approx 9.0$ to $W_c \approx 2.14$), the underlying critical physics governing the transition remains invariant once the symmetry is broken.
3. *Methodological Advancement:* The LNS method presented here establishes a new standard for numerical studies in non-Hermitian physics, offering a stable route to analyze phase transitions in large-scale systems.

These findings suggest that the universality class identified here is likely the fundamental description for 1D non-Hermitian Anderson transitions. Future work may extend this high-precision approach to study the interplay of this universality with many-body interactions or higher-dimensional non-Hermitian lattices.

ACKNOWLEDGMENTS

This work made extensive use of the open-source Python scientific computing ecosystem, including NumPy, SciPy, and Matplotlib. The numerical stability required to achieve the thermodynamic limit ($N > 1000$) was specifically realized through the Log-Space Non-Hermitian Scaling (LNS) method developed herein.

Generative AI tools were employed solely for language editing and stylistic support during manuscript preparation; no AI systems were involved in data analysis, figure generation, or physical interpretation of the results**.** All processed data (CSV and NPZ files), final figure assets, and Python scripts used for simulations and figure generation are provided in the supplementary ZIP archive. In addition, the complete raw datasets and primary source codes are made available as code-repo.rar for reproducibility and independent verification.

APPENDIX A: THE LOG-SPACE NON-HERMITIAN SCALING (LNS) METHOD

In non-Hermitian systems exhibiting the skin effect, the transmittance T scales exponentially with system size L, i.e., $T \sim e^{2\gamma L}$. For the parameters used in this study ($L = 1200, \gamma = 0.6$), T exceeds 10^{600}, surpassing the IEEE 754 double-precision limit ($\approx 10^{308}$). Here, we derive the Log-Space Non-Hermitian Scaling (LNS) formalism used to compute the Lyapunov exponents without numerical overflow.

1. Log-Space Caroli Formulation

The transmittance $T(E)$ across a 1D chain connected to semi-infinite leads is given by the Caroli formula [16]:

$$T(E) = 4\sin(k_L)\sin(k_R)\left|G_{1,N}(E)\right|^2$$

where $k_{L,R} = \arccos\big((E \pm i\eta)/2t\big)$ are the lead momenta (assuming symmetric leads $t_L = t_R = t$), and $G_{1,N}$ is the corner element of the retarded Green's function $G^r = \left(E - H_{eff}\right)^{-1}$. The effective Hamiltonian H_{eff} includes the non-Hermitian self-energies $\Sigma_{L,R}$ at the boundaries.

Instead of computing T directly, we define the logarithmic transmittance $\mathcal{L}_{\mathcal{T}}$:

$$\mathcal{L}_{\mathcal{T}} = \ln T\,(E) = \ln(4|\sin k_L||\sin k_R|) + 2\ln\left|G_{1,N}\right|$$

The Green's function element $G_{1,N}$ is computed via standard matrix inversion. Crucially, the magnitude is immediately converted to the logarithmic domain [15,16]:

$$\ln\left|G_{1,N}\right| = \frac{1}{2}\ln\left(\mathrm{Re}\left[G_{1,N}\right]^2 + \mathrm{Im}\left[G_{1,N}\right]^2\right)$$

This operation ensures that all subsequent operations remain within the stable range of floating-point arithmetic.

2. The Log-Difference Algorithm (Stable Subtraction)

The central quantity for the Anderson transition is the Lyapunov exponent $\lambda(E)$, often derived from the asymmetry of transmittance or the geometric mean. For the delocalization index, we require the magnitude of the difference between forward ($T_{\rightarrow}$) and backward ($T_{\leftarrow}$) transmittance:

$$\Delta T = |T_{\rightarrow} - T_{\leftarrow}|$$

Directly computing this difference is impossible when $T_{\rightarrow} \approx e^{1000}$. We therefore compute the logarithm of the magnitude of the difference, $\mathcal{L}_{\Delta} = \ln(|\Delta T|)$, using the Log-Space Subtraction (LSS) technique. Let $x = \mathcal{L}_{\mathcal{T}_{\rightarrow}}$ and $y = \mathcal{L}_{\mathcal{T}_{\leftarrow}}$. Assuming $x \geq y$ without loss of generality, we factor out the larger exponential term, e^x:

$$\Delta T = e^x - e^y = e^x(1 - e^{y-x})$$

Taking the logarithm of the magnitude of both sides yields the final computationally stable form:

$$\mathcal{L}_{\Delta} = x + \ln|1 - \exp(y - x)|$$

Since $x \geq y$, the term $y - x$ is always non-positive, ensuring that $\exp(y - x) \in [0,1]$. This formulation allows the precise evaluation of the difference between two astronomically large numbers without exceeding the limits of floating-point arithmetic. The Lyapunov

*Contact author: tozarali@mku.edu.tr

exponent is then obtained from the normalized logarithmic difference:

$$\lambda = \lim_{L\to\infty} \frac{1}{L} \ln(|\Delta T|) \approx \frac{\mathcal{L}_\Delta}{L}$$

.

APPENDIX B: DISORDER MODELS AND HAMILTONIANS

We provide the explicit matrix forms of the Hamiltonians used in the FSS analysis to ensure reproducibility. The system is a 1D chain of L sites with open boundary conditions.

1. Uniform and Binary Models (Diagonal Disorder)

For these models, the hopping is uniform, and randomness is in the diagonal terms:

$$H_{nm} = \delta_{n,m+1} t e^{-\gamma} + \delta_{n,m-1} t e^{\gamma} + \delta_{nm} V_n$$

- *Uniform:* $V_n \sim \mathcal{U}[-W/2, W/2]$ (Continuous box distribution).
- *Binary:* $V_n \in \{-W/2, +W/2\}$ with $P = 0.5$ (Discrete distribution).

2. Off-Diagonal Model (Random Hopping)

Here, the diagonal potential is strictly zero ($V_n = 0$), preserving chiral symmetry at $E = 0$. Randomness is introduced in the hopping amplitudes t_n:

$$H_{nm} = \delta_{n,m+1} t_m e^{-\gamma} + \delta_{n,m-1} t_n e^{\gamma}$$

where $t_n = t + \delta_n$ with $\delta_n \sim \mathcal{U}[-W/2, W/2]$. The modulation of t_n affects both forward and backward hopping simultaneously, maintaining the non-Hermitian reciprocity relation $H_{nm}/H_{mn} = e^{2\gamma}$ locally.

.

References

[1] E. Abrahams, P. W. Anderson, D. C. Licciardello, and T. V. Ramakrishnan, Phys. Rev. Lett. 42, 673 (1979).

[2] N. Hatano and D. R. Nelson, Phys. Rev. Lett. 77, 570 (1996).

[3] C. M. Bender and S. Boettcher, Phys. Rev. Lett. 80, 5243 (1998).

[4] C. M. Bender, Reports on Progress in Physics 70, 947 (2007).

[5] Z. Gong, Y. Ashida, K. Kawabata, K. Takasan, S. Higashikawa, and M. Ueda, Physical Review X 8, 031079 (2018).

[6] H. Shen, B. Zhen, and L. Fu, Phys. Rev. Lett. 120, 146402 (2018).

[7] K. Kawabata, S. Higashikawa, Z. Gong, Y. Ashida, and M. Ueda, Nature Communications 10, 297 (2019).

[8] X. Zhang, T. Zhang, M.-H. Lu, and Y.-F. Chen, Advances in Physics: X 7, 2109431 (2022).

[9] L. Xiao, T. Deng, K. Wang, G. Zhu, Z. Wang, W. Yi, and P. Xue, Nature Physics 16, 761 (2020).

[10] X. Luo, T. Ohtsuki, and R. Shindou, Physical Review B 104, 104203 (2021).

[11] R. Sarkar, S. S. Hegde, and A. Narayan, Physical Review B 106, 014207 (2022).

[12] K. Kawabata, K. Shiozaki, M. Ueda, and M. Sato, Physical Review X 9, 041015 (2019).

[13] X. Luo, T. Ohtsuki, and R. Shindou, Phys. Rev. Lett. 126, 090402 (2021).

[14] A. Tozar, Universal Critical Scaling and Phase Diagram of the Non-Hermitian Skin Effect under Disorder, 2025.

[15] S. Datta, Electronic Transport in Mesoscopic Systems (Cambridge University Press, Cambridge, 1995), Cambridge Studies in Semiconductor Physics and Microelectronic Engineering.

[16] C. Caroli, R. Combescot, P. Nozieres, and D. Saint-James, Journal of Physics C: Solid State Physics 4, 916 (1971).

[17] E. N. Economou, Green's Functions in Quantum Physics (Springer Berlin, Heidelberg, Berlin, Heidelberg, 2006), 3 edn., Vol. 7, p.^pp. Springer Series in Solid-State Sciences.

[18] P. Blanchard, D. J. Higham, and N. J. Higham, IMA Journal of Numerical Analysis 41, 2311 (2021).

[19] F. J. Dyson, Physical Review 92, 1331 (1953).

[20] K. Binder and D. P. Landau, Physical Review B 30, 1477 (1984).

[21] R. Hamazaki, K. Kawabata, and M. Ueda, Phys. Rev. Lett. 123, 090603 (2019).

[22] A. B. Culver, P. Sathe, A. Brown, F. Harper, and R. Roy, Physical Review B 112, 104205 (2025).

*Contact author: tozarali@mku.edu.tr